JKAU: Eng. Sci., **Vol. 18** No. 2, pp: 101-122 (2007 A.D. /1428 A.H.)

Analysis of the Turbulent Flow and Heat Transfer of the Impingement Cooling in a Channel with Cross Flow

Khudheyer S. Mushatat

College of Engineering, Thiqar University, Nassiriya, Iraq
Khudheyer2004@yahoo.com

Abstract. In this paper, a numerical study to analyze the turbulent flow and heat transfer characteristics of the impinging slot jets in a channel with cross flow has been carried out. For this flow configuration, two cases were considered for the channel, one without ribs and the other with rib turbulators. The characteristics of air flow and heat transfer are analyzed under different parameters such as the size of the jets, the number of jets and ribs, arrangement of jets and ribs, the pitch between the jets and jet Reynolds number. An implicit finite volume scheme has been used to integrate the continuity, elliptic Reynolds average Navier-Stockes and energy equation giving a set of equations valid for the entire computational domain. Turbulence effects are modeled using a k-ϵ model. The wall effects are modeled using a wall function approach. The obtained results show that the recirculation regions, the local Nusselt number variation, and the turbulent kinetic energy are greatly effected with the size of jets and ribs, the distance between the jets, rib thickness and jet Reynolds number. Also the results indicate that the ribs arrangement with respect to impinging slot jets has a significant effect on the heat transfer enhancement. The validation of the present code is done by comparing the present results with the available published experimental results.

1. Introduction

Jet impinging cooling has been used for many industrial and engineering applications such as cooling of gas turbine blades, cooling of electronic components, tempering of glass and drying of papers. Impinging jets has received considerable attention because they can remove a large amounts of heat over a small area consequently producing high local heat transfer. In some applications of impinging cooling, slot jets are superior to circular jets since a slot jet has a large impingement region. The increase of the distance between the jet and the surface leads to decreasing the local heat transfer significantly, so the remedy is adopting a multiple

impinging jets or using a rib roughened walls. Thus it is important to show the effect of the rib turbulators on the flow field and impinging heat transfer. Concerning slot impinging jets, extensive experimental and numerical studies has been conducted. Law and Masliyah [1], Chou and Hung [2] and Lee *et al*. [3] performed numerical investigations on low Reynolds number impinging jets. The cause behind using low Reynolds number was to avoid a hydrodynamic pressure caused by the impinging on the surface. Benna *et al*. [4], Park and Sung [5] and Cooper *et al*. [6] presented numerical studies on high Reynolds number impinging jets with different turbulenc models. To improve heat transfer distribution in the impingement region, impinging jets were studied with different angles of attacks. Beitelmal *et al*. [7], Yang and shyu [8] and Gabry *et al*. [9] used CFD models to predict the heat transfer distribution on a smooth surface under an array of angled impinging jets with cross flow. Different angles of attack and conjugate conduction in the boundary were included. The k-ϵ model and yang-Shih model were examined. The study showed that yang-Shih model superior to k-ϵ. Craft *et al*. [10] applied four turbulence models to the numerical prediction of the turbulent impinging jets discharged from a circular pipe. Shou *et al.* [11] studied the effect of jets in cross flow on impingement heat transfer from rib-roughened rotating curved square duct. The curvature of the duct, rib height, pitch to height ratio (p/e) was fixed while the jet Reynolds and stream cross flow were changed. Concerning the flow and heat transfer characteristics inside a channel roughened with rib turbulators, Web *et al*. [12], Lio and chen [13] and Rau *et al.* [14] and Hane and Park [15] studied the turbulent flow and heat transfer. The main objective of these studies was to obtain the heat transfer characteristics and friction factor. Saidi and Sunden [16] investigated the turbulent flow and heat transfer in three dimensional rib-roughened channels using a simple eddy viscosity model and algebraic stress model. Their study showed that the algebraic stress model has superiority over the eddy viscosity model for the prediction of the flow field but the mean thermal predictions are not very different. Also Viswanathan and Tafti [17-18], Murata and Mochizulki [19] and Watanabi and Takahashi [20] studied the turbulent flow in the channels roughened with ribs.

In this work, a numerical study to predict the turbulent flow and heat transfer of multiple impinging slot jets in a cross channel flow has been performed. Two cases were considered regarding the channel cross flow, one the channel is free ribs and the other is the channel roughened with ribs. As shown in Fig. 1, the jet has a width (B), the rib has a

thickness (W), the height of the channel is (H). The channel height to a jet width ratio (H/B) and the jet width to the rib thickness ratio(B/W) are changed for different values. Different jet Reynolds numbers and a channel cross flow Reynolds numbers are examined. The jet Reynolds number is based on the jet width (B) and the channel Reynolds number on the channel height(H). The effect of the location of the impinging jets with respect to the ribs on heat transfer is investigated. The objective of this investigation is to determine the flow and heat transfer characteristics of the confined impingement cooling and to show how the turbulent cooling affected impinging cooling in a rib roughened channel.

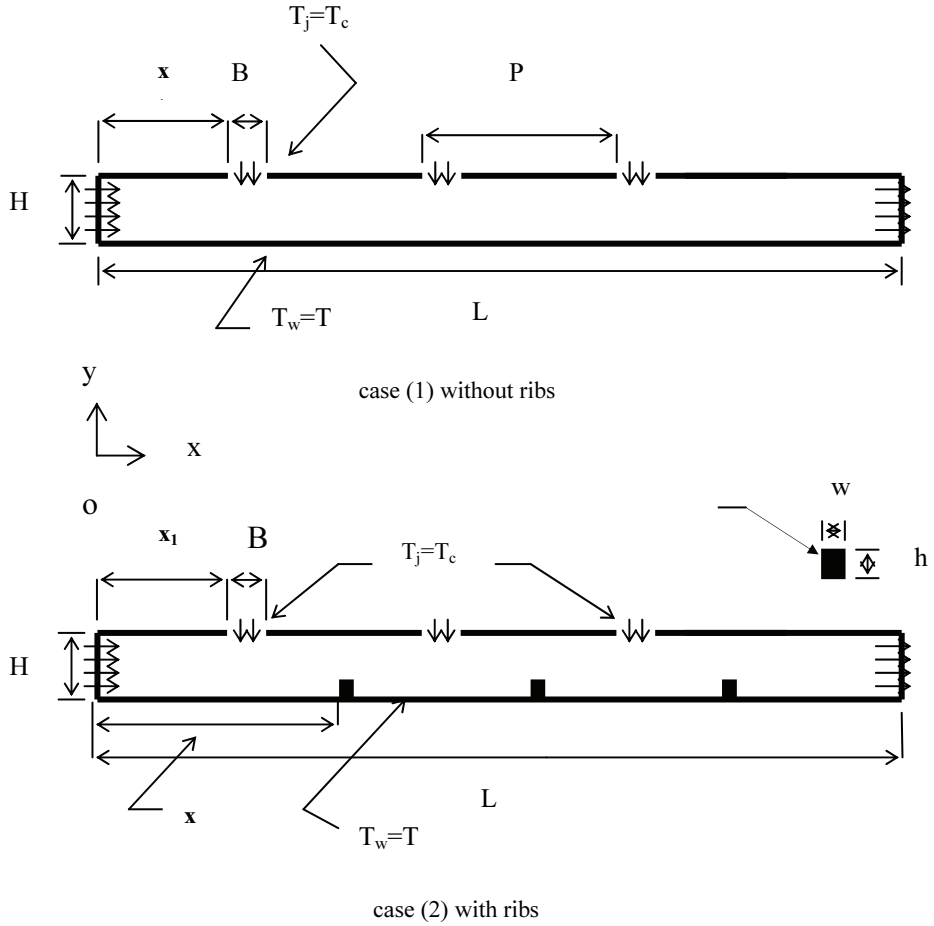

Fig.1. Problem description with H=0.05 m, L=0.4 m, H/B=11, h/H=0.38, W/h=2, P/B=4, x_1=0.0492m, x_2=0.0826m, e=0.11m

2. Mathematical Model

The turbulent Navier-Stockes and energy equations are solved numerically along with the continuity equation to simulate the flow and thermal fields. To simplify the numerical simulation by using a two dimensional mathematical model (with finite volume scheme), the flow properties are assumed constant and Boussinesq approximation is valid. The Reynolds average Navier-Stokes and energy equations in tensor form can be written as:

$$\frac{\partial}{\partial x_i}\left(\rho U_i\right)=0 \tag{1}$$

$$\frac{\partial U_i U_j}{\partial x_j} = \frac{-\partial P}{\partial x_i}+\frac{\partial}{\partial x_j}\left(\mu\frac{\partial U_i}{\partial x_j}-\overline{\rho u_i u_j}\right) \tag{2}$$

$$\frac{\partial U_i T_j}{\partial x_j} = \frac{\partial}{\partial x_j}\left(\frac{\mu}{\Pr}\frac{\partial T_i}{\partial x_j}-\overline{\rho u_i t_j}\right) \tag{3}$$

The turbulent stresses $\overline{\rho u_i u_j}$ and turbulent heat fluxes $\overline{\rho u_i t_j}$ should be modeled in order to close the considered governing equations. One of the most widely turbulence models is the standard k-ϵ model. This model has the ability to handle complex high Reynolds number flows in much less time than other complicated models. This model solves two transport equations one for the turbulent kinetic energy and the other for the dissipation rate of the turbulent kinetic energy [22] as shown below:

$$\frac{\partial \rho k U_i}{\partial x_j}=\frac{\partial}{\partial x_j}\left[\left(\mu+\frac{\mu_t}{\sigma_k}\right)\frac{\partial k}{\partial x_j}\right]+\rho\left(G_b-\varepsilon\right) \tag{4}$$

$$\frac{\partial \rho \varepsilon U_j}{\partial x_j}=\frac{\partial}{\partial x_j}\left[\left(\mu+\frac{\mu_t}{\sigma_\varepsilon}\right)\frac{\partial \varepsilon}{\partial x_j}\right]+\rho\frac{\varepsilon}{k}\left(C_{1\varepsilon}G_b-C_{2\varepsilon}\varepsilon\right) \tag{5}$$

where the shear production term, (G_b) is defined as:

$$G_b=\mu_t\left(\frac{\partial u_i}{\partial x_j}+\frac{\partial u_j}{\partial x_i}\right)\frac{\partial u_i}{\partial x_j} \tag{6}$$

and the turbulent viscosity is defined as:

$$\mu_t = \rho c_\mu \frac{k^2}{\varepsilon} \tag{7}$$

the model coefficients are (σ_k ;σ_ϵ ; $C_{1\epsilon}$; $C_{2\epsilon}$; $C\mu$) = (1.0, 1.3, 1.44, 1.92, 0.09) respectively. The flow parameters at inlet are described as follows:

$k_{in} = 1.5 I_u^{\,2} U_{in}^{\,2}$, $k_j = 1.5 I_u^{\,2} U_j^{\,2}$, $I_u = 2\%$

$\varepsilon_{in} = k_{in}^{\,1.5} \,/\, \lambda H$, $\varepsilon_j = k_j^{\,1.5} \,/\, \lambda B$, $\lambda = 0.005$

$\mathrm{Re}_{in} = \frac{U_{in} H}{\nu}$, $\mathrm{Re}_j = \frac{U_j B}{\nu}$, $T_{in} = T_c = 25\dot{\mathrm{C}}, T_j = T_c = 25\ \dot{\mathrm{C}}$,

where k_{in}, k_j, U_{in}, U_j, T_{in}, T_j are the turbulent kinetic energy, velocity and temperature at a channel inlet and a slot jet respectively.

At the walls, no slip conditions are imposed; U=V=0., k = 0, $\frac{\partial \varepsilon}{\partial y} = 0$, $T_w = T_h$=50 $\dot{\mathrm{C}}$. While T_c=25 $\dot{\mathrm{C}}$ is assigned to the rib turbulators. The local Nu along the bottom hot wall is expressed as $Nu = \frac{\partial \theta}{\partial Y}$, at

$$\mathrm{y} = 0\ ,\ \theta = \frac{T - T_c}{T_h - T_c},\ Y = \frac{y}{H}$$

To obtain a smooth transition at the channel exit, the second derivative of the considered dependent variables is equal to zero (*i.e.*, $\frac{\partial^2 U}{\partial x^2} = 0$,…, *etc*). To remedy the large steep gradients near the walls of the channel and the rib turbulators, there are two approaches. In the first approach, the turbulence model is modified to enable this region to be resolved with a fine mesh. In the second approach, the wall function approximation used by Versteege [23] is used to handle the mean velocities, temperature along with the formulas of near wall turbulence quantities. This approach is adopted here because it is economical, popular, reasonably accurate and saves computational resources.

3. Numerical Procedure

In this study, the numerical computations are performed on non-uniform staggered grid system. A finite volume method (FVM) described by the following formula is adopted to integrate the considered governing equations (1) to (5).

$$\int_{cv}(\rho\phi u)dv = \int_{cv} div(\Gamma grad\phi)dv + \int_{cv} S_\phi dv \qquad (8)$$

This gives a system of discretization equations which means that the system of elliptic partial differential equations is transformed in to a system of algebraic equations. Then the solution of these transformed equations is performed by implicit line by line Guass elimination scheme. An elliptic finite volume computer code is developed to attain the results of the numerical procedure through using pressure-velocity coupling (SIMPLE algorithm) [23]. This code is based on hybrid scheme. Due to this strong inherent coupling and non-linearity inherent in these equations, relaxation factors are needed to ensure convergence. The relaxation factors used for velocity components, pressure , temperature and turbulence quantities are 0.5, 1, 0.7, 0.7 respectively. However these relaxation factors have been adjusted for each case studied to accelerate the convergence criterion defined as the relative deference of every dependent variable between iteration steps. A typical run of 5000 takes about 215 CPU seconds on PENTIUM 4 computer is done. To ensure that the turbulent fluid flow solutions are not significantly affected by the mesh, the numerical simulations are examined under different grid sizes ranging from (62×28) until (82×52) control volumes. Any additional increase in grid points on (62×28) does not significantly effect the results.

4. Results and discussions

Figure 2 demonstrates the distribution of computed velocity vectors for multiple impinging slot jets in a cross flow. It is clear that the recirculation regions formed between the jets and re-attachment length are increased with the increase of the number of jets. As the Figure shows, the cross flow affect the behavior and trajectories of multiple impinging jets in which the potential core region of each jet is distorted. A part of the flow of impinging jets forms re-circulating regions between the jets and the other part push the cross flow towards the wall of the channel consequently the main flow is accelerated and the channel flow passage becomes narrower. This situation will enhance the heat transfer as shown in the next sections.

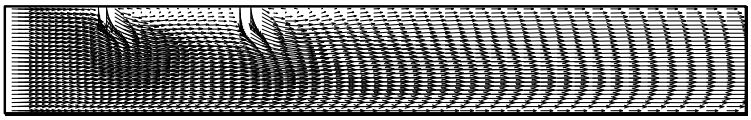

(a) Two jets

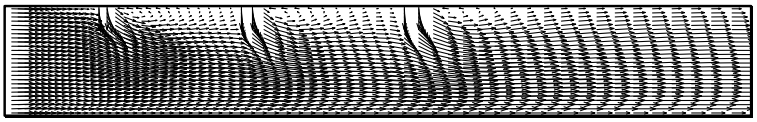

(b) Three jets

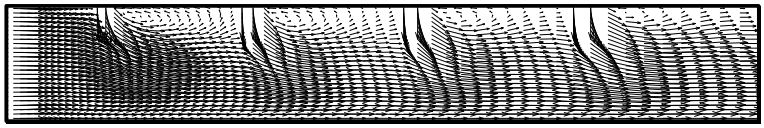

(c) Four jets

Fig. 2. Computed velocity vectors for multiple impinging iets in cross flow.

Figures 3&4 exhibit the effect of the ratio of the channel height to the slot jet width (H/B) on the computed flow field. It is evident that the recirculation regions behind each jet are increased with the increase of the slot jet width (i.e. decreasing the ratio H/B). This flow structure is dominant for all the studied cases. The flow of impinging jets strongly affected the main cross stream when H/B=2.5 for all the studied cases. However this situation is tested here for the considered number of jets in this study . In general, the velocity of the main channel flow near the hot wall is increased with decreasing the ratio H/B (increasing the width of the impinging jet) since the channel becomes narrower. This shrinking will increase the velocity gradient in the vicinity of the wall consequently increasing the shear stresses. When the velocity gradients are increased, the turbulence effects are increased and this has a direct effect on the enhancement of heat transfer as shown in the next sections.

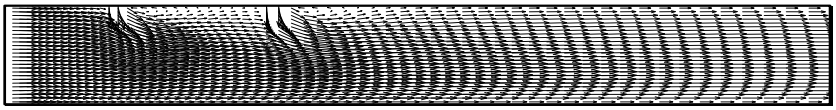

(a) H/B=11

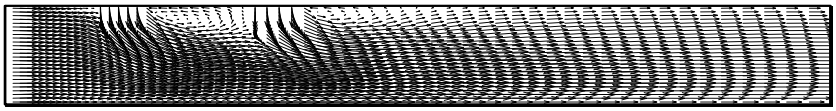

(b) H/B=2.5

Fig. 3. Effect of a slot jet width on the flow field for 2 slot jets, Re_j =13517, Re_{in}= 16896 P/B=4.

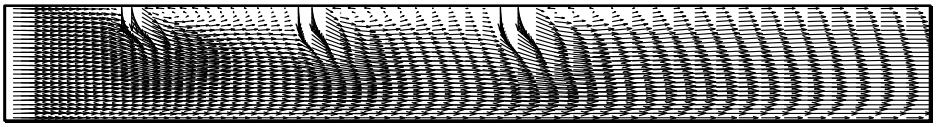

(a) H/B=11

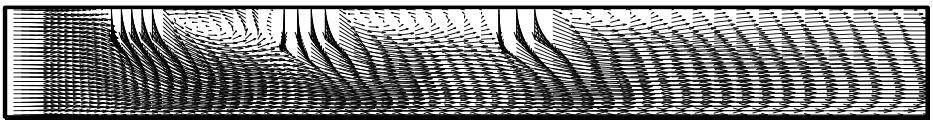

(b) H/B=2.5

Fig. 4. Effect of a slot jet width on the flow field for 3 slot jets, Re_j =13517, Re_{in}= 16896, P/B=4.

The effect of the ratio of the channel height to the impinging slot jet width (H/B) on the distribution of a local Nusselt number is depicted in Fig.5. It can be seen that the local Nusselt number is increased with the increase of a jet width (decreasing the ratio H/B). The reason behind this is that the recirculation regions are increased behind each jet and that leads to increasing the impinging flow towards the hot wall along with increasing the turbulence effects, consequently increasing the heat transfer enhancement as shown in (b) and (c). This situation can be achieved for all studied number of jets as shown in (a).

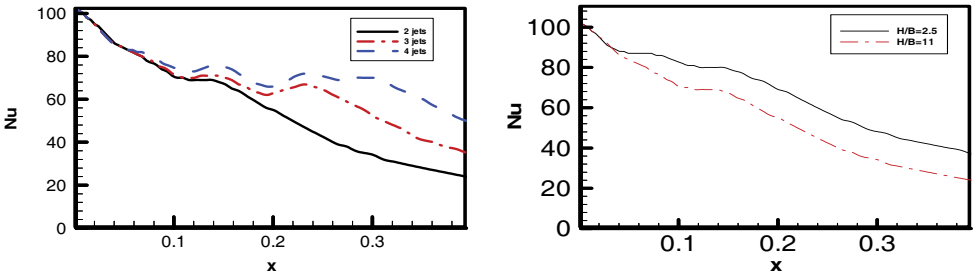

(a) multiple jets with (b) 2 jets

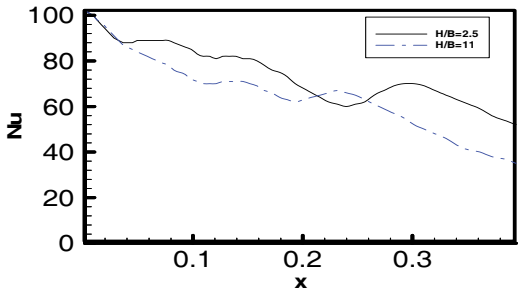

(c) 3

Fig. 5. Effect of a slot jet width on Nusselt number variation, Re_j =13517, Re_{in}= 16896, P/B=4.

The effect of the pitch to the jet width ratio (P/B) on the computed velocity vectors is depicted in Fig. 6. As velocity vectors, case (a) and case (b), it can be seen that the recirculation regions are decreased with increasing the ratio (P/B), although the cooling of the wall in the first jet at (P/B) = 4 is stronger. The trajectories of the impinging jets forced the cross flow towards the wall under impinging areas and between the jets are clearly seen in case (b) and case (d). The streamlines are seen to be deflected more toward the wall in case (c) rather than case (d). However this increase becomes less down stream the second jet. This behavior explain the variation of the Nusselt number in case (e) where the values of Nusselt number are higher at the region included by the effect of closely spaced two jets while this behavior is changed when reaching the second jet at P/B=12.

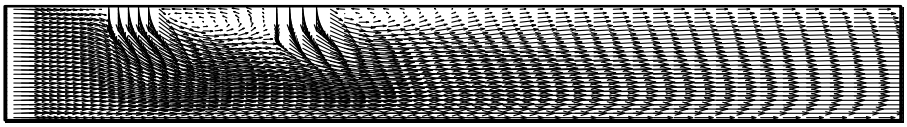

(a) Velocity vectors for P/B=4

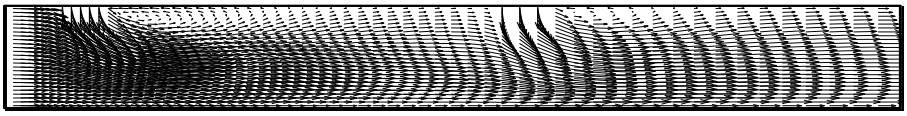

(b) Velocity vectors for P/B=12, x_1=0.024m

(c) Streamlines for P/B=4

(d) Streamlines for P/B=12, x_1=0.024m

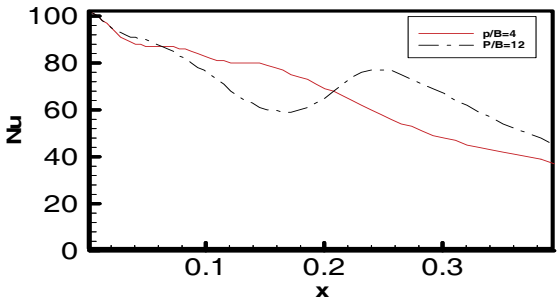

(e) Nusselt number variation

Fig. 6. Effect of the distance between the jets on the flow and heat Characteristics, Re_{in}= 16896, Re_j =13517, H/B= 2.5.

The recirculation zone behind each jet and reattachment length are significantly increased with the increase of the impinging slot jet velocity and cross stream velocity (*i.e.*, Re_j and Re_{in}) as shown in Fig. 7. The

increase in Reynolds number increase the inertia force and the penetration of the impinging jet flow to the cross flow and consequently enhance heat transfer as shown in Fig.8. This fact is dominant for all studied cases.

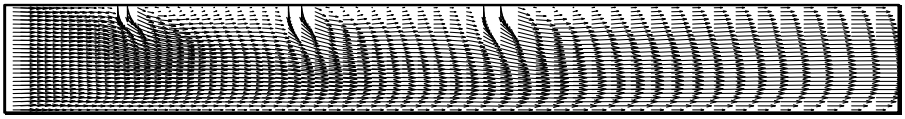

(a) Rej=6210.

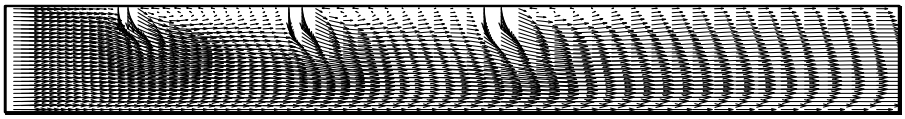

(b) Rej=13517

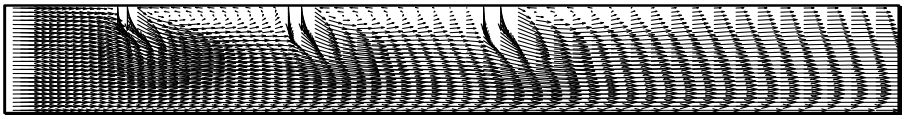

(c) Rej=28127.

Fig. 7. Effect of Reynolds number on the computed flow field for 3 jets, H/B=11, P/B=4, Re_{in}= 16896

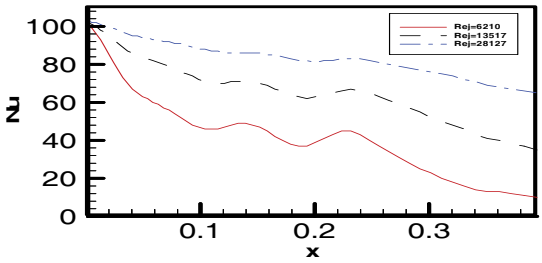

Fig. 8. Effect of Reynolds number on Nusselt number for 3 jets, H/B=11, P/B=4.

The distribution of the turbulent kinetic energy of multiple impinging jets in confined cross flow is depicted in Fig. 9 It is clear that the turbulent kinetic energy is increased with the increase of the number of jets. In all studied cases the increase in kinetic energy is concentrated

in recirculation flows and the impinging jets flows because the turbulence is higher than the other regions of this complex flow.

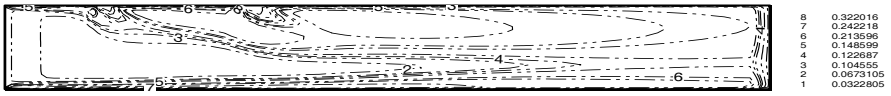

(a) 2 jets

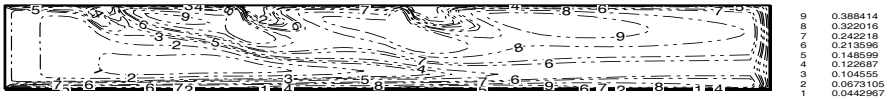

(b) 3 jets

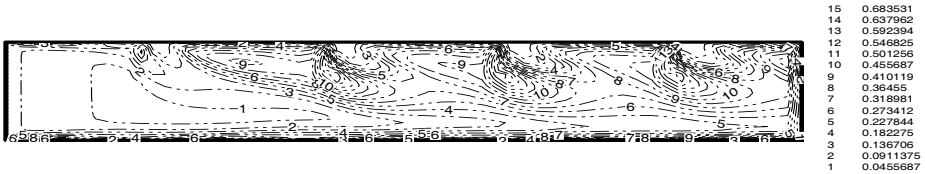

(c) 4 jets

Fig. 9. Contours of turbulent kinetic energy, Re_j =13517, P/B=4, H/B=11, Re_{in}= 16896.

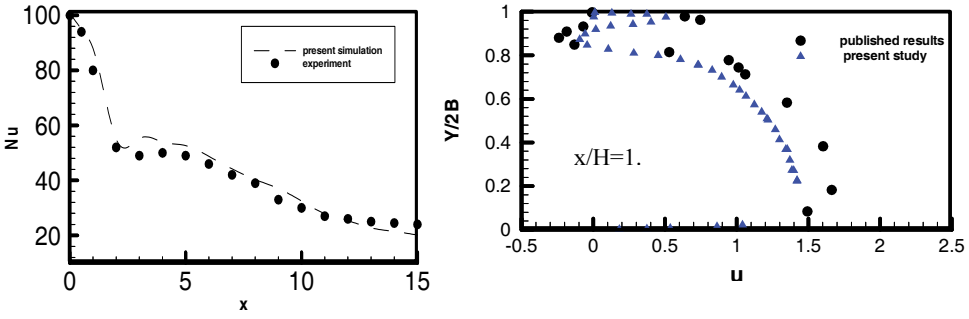

(a) Impinging cooling, one jet [21], H/B=1, Re_j=6000

(b) Published results of Lio *et al*.[13], turbulent cooling, H/B=1, Re=6000.

Fig. 10. Comparison between the present simulation and published experimental data.

The validation of the present code is examined through the comparison of the present results with available published experimental

results as shown in Fig. 10. The comparison indicated acceptable agreement. The effect of the presence of rib turbulators on impinging jet cooling in cross channel flow is exhibited as a stream line contours in Fig.11. As the Figure shows one might see that the recirculation regions and reattachment length behind each jet are decreased while new recirculation regions and separation of boundary layer are shown due to the existence of ribs. It can be seen here that the recirculation regions between the impinging slot jets are significantly decreased . This is because of the presence of ribs. The impinging jet flows and the cross flow cannot deflect directly towards the hot wall where the ribs shift the combined flow and accelerates it down stream the rib forming a recirculation zone. This will enhance heat transfer too. Thus the presence of ribs has merits and disadvantages. As the figure shows, the increase of the number of ribs increases the turbulence along with the increase of multiple impinging jets as shown in (a, b, c). This is expected to enhance the heat transfer because the turbulence is higher in this combined complex flow. The presence of rib prevents the deflection of high inertia flow (cross flow plus jet flow) towards the hot wall, but the deflection of stream lines occurs at regions between the ribs. The flow is faster above and down stream each rib.

(a) 2 jets

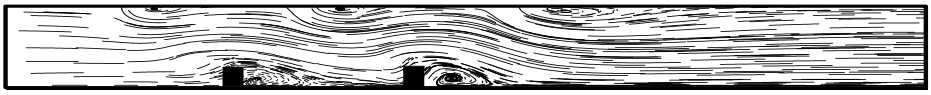

(b) 3 jets

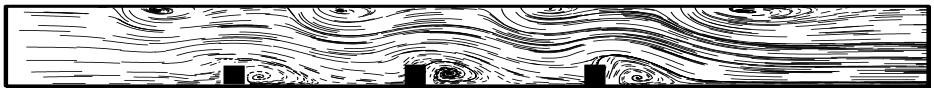

(c) 4 jets

Fig. 11. Stream lines of multiple impinging jets with ribs, H/B=11, B/W=1, h/W=2, h/H=0.38, Re_{in}= 16896, Re_j =13517.

Figure 12 demonstrates the velocity vectors and streamlines contour of multiple impinging jets in a rib roughened channel. The ratio of the channel height to the jet width is decreased to 2.5 and the ratio of the jet width to the rib thickness is decreased to 2. As the figure shows, these ratios have a strong effect on the recirculation regions and reattachment length with regard to the impinging cooling and turbulent cooling. The recirculation regions behind the ribs and jets are noticeably increased. However this increase is larger at the turbulent cooling rather than the impinging cooling. For this combined complex flow, the main flow penetration to the hot wall seems to be stronger and the heat transfer is enhanced as shown in Fig. 14. This occurs as a result to increase the mass flow rate of the flow of impinging jets. However the increase of the recirculation regions size between the impinging slot does not reach the recirculation regions in size in the case of the channel without ribs. As a result we expect a heat transfer enhancement is better as shown in Fig.13.

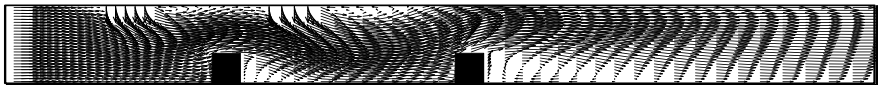

(a) 2 jets for H/B=2.5

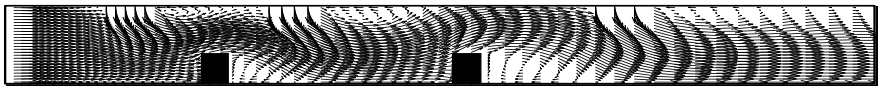

(b) 3 jets for H/B=2.5, B/W=2

(c) streamlines for 2 jets and H/B=2.5, B/W=2

(d) streamlines for 3 jets and H/B=2.5, B/W=2

Fig. 12. Velocity vectors and streamlines for Re_j=13517 and Re_{in}= 16896.

The effect of the number of impinging slot jets on a local Nu variation is seen in Fig13. The figure shows that the Nu is decreased with the increase of the number of jets.

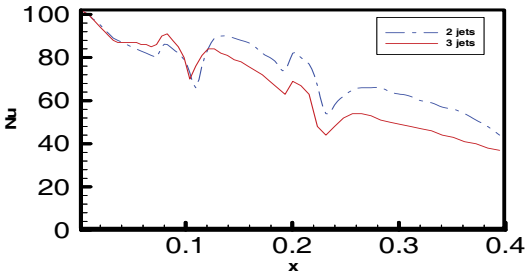

Fig. 13. Variation of Nusselt number in cross flow with ribs (H/B=2.5, B/W=2, Re_j=13517 and Re_{in}= 16896).

The effect of decreasing the ratios (H/B) and increasing the ratio (B/W) on the variation of a local Nu is depicted in Fig. 14. It can be seen that the presence of ribs increased the Nu number because the ribs increase the resultant turbulence and promote the heat exchange with the hot wall and consequently enhance the heat transfer. This situation is dominant for all studied cases. Fig.15 demonstrates the variation of local Nusselt number for the considered studied cases. It can be seen that the local Nusselt number is increased significantly with the presence of rib turbulators. However this behavior is decreased at the last stream stations of the channel when the number of jets equals four. This may be due to the presence of the four jets near the channel exit and there is no enough heat exchange with the area near the hot wall.

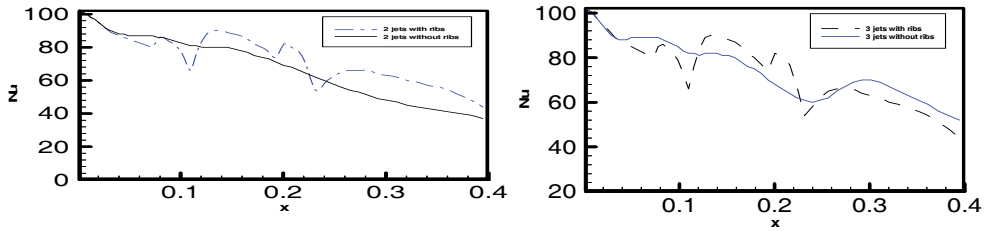

(a) (b)

Fig. 14. Comparison of Nu number in cross flow with and without ribs, H/B=2.5, B/W=2, Re_i=13517 and Re_{in}= 16896.

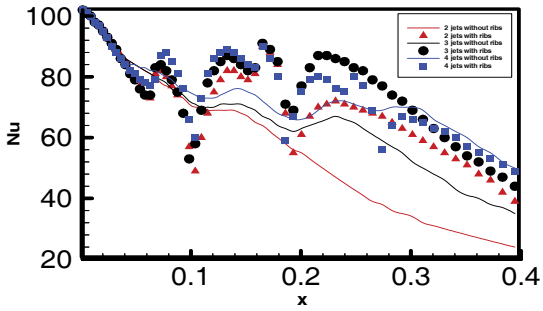

Fig. 15. Local Nusselt number variation, H/B=11, B/W=1, Re_j=13517 and Re_{in}= 16896.

The distribution of the turbulent kinetic energy for impinging jet cooling in a channel roughened with ribs is found in Fig.16. It can be seen that the turbulent kinetic energy is decreased with the increase of the number of jets. Also it can be seen there is a significant increase in a turbulent kinetic energy in the presence of ribs compared with the case of no ribs. Also the velocity gradient is less at the flow exit so the kinetic energy is rapidly decreased.

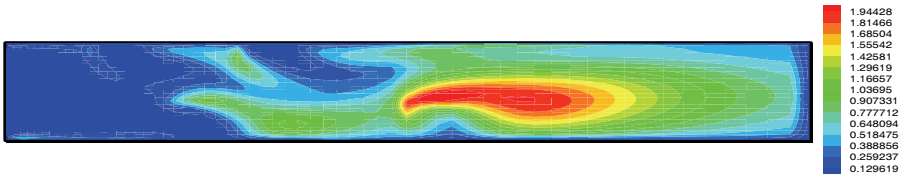

(a) 2 jets, H/B=11, B/W=1

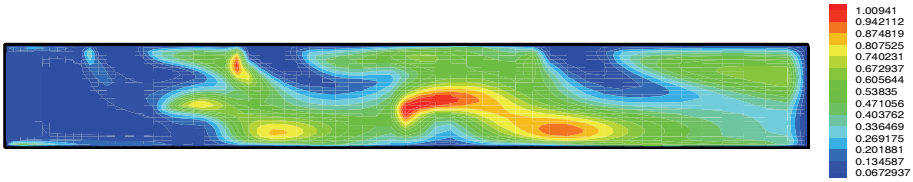

(b) 3 jets, H/B=11, B/W=1

Fig.16. Turbulent kinetic energy distribution with ribs, Re_j=13517 and Re_{in}= 16896.

To increase the recirculation regions between the impinging slot jets, an attempt is made to change the arrangements of rib turbulators. The ribs are placed just below the impinging slot jets. As a result, the heat transfer is enhanced as shown in Fig.17. The cause behind this is when the ribs are replaced between the jets, the recirculation regions are decreased and the deflected flow is prevented from approaching the hot wall.

(a) 3 jets

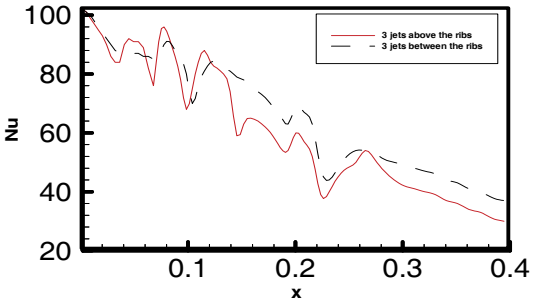

(b) 4 jets

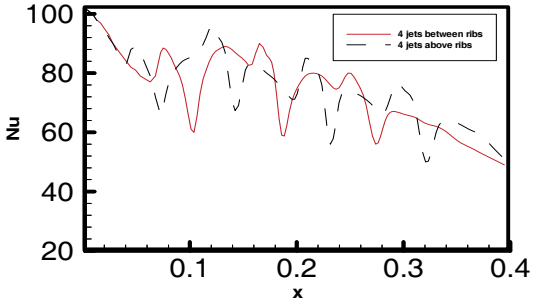

Fig.17. Effect of rib location on Nusselt number variation, Re_j=13517 and Re_{in}= 16896.

Figure 18 demonstrates the effect of increasing the grid nodes on the distribution of the flow field and Nussult number for three impinging cooling jets. It can be seen that the flow field and Nusselt number are not greatly effected when the mesh exceeding (62×28 node) along with adopting the wall function approximations.

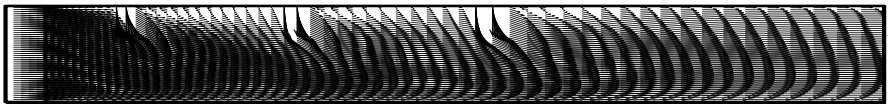

(a) flow field, mesh= 62×52

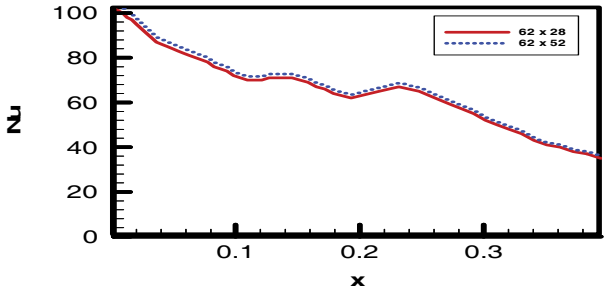

(b) Nu variation for three impinging slot jets

Fig. 18. Effect of increasing grid nodes on the studied variables, H/B=11, P/B=4, Re_i=13517 and Re_{in}= 16896.

5. Conclusions

The standard k-ϵ model with finite volume techniques has been proved effectively to simulate the turbulent flow and heat transfer of the impinging cooling and turbulent cooling in channels. The large recirculation regions induced by both impinging slot jets and rib turbulators result in high heat transfer enhancement. The arrangement of ribs with respect to jets positions has a great effect on the size of the recirculation regions induced by jets consequently on heat transfer enhancement. The local Nusselt number and the size of the recirculation zones are increased with the increase of (B/W) and decrease of (H/B). The study shows that the number of impinging slot jets and ribs has a profound effect on the flow field , heat transfer characteristics and turbulent kinetic energy.

Notations

B = slot jet width [m]
e = distance between ribs [m]
h = rib height [m]
H = channel height [m]

i, j = tensor notation
I_u = turbulence intensity
k = turbulent kinetic energy [m^2/s^2]
Nu = local Nusselt number
P = jet pitch [m]
p = pressure [N/m^2]
Pr = Prandtl number
Re = Reynolds number
T = temperature [Ċ]
T_c = cold temperature [Ċ]
T_h = hot temperature [Ċ]
T_w = hot wall temperature [Ċ]
$\overline{\rho u_i u_j}$ = Reynolds stresses [kg/ms^2]
$\overline{\rho u_i t_j}$ = turbulent heat fluxes [Kg Ċ/m^2s]
U_{in} = velocity at a channel inlet [m/s]
U_j = velocity at a slot jet inlet [m/s]
W = rib thickness [m]
x, y = cartesian coordinates [m]
Y = dimensionless y-axis coordinate

Greek symbols:
μ = molecular viscosity [kg/ms]
μ_t = turbulent viscosity [Kg/ms]
ρ = air density [Kg/m^3]
σ_k = turbulent Prandtl number for turbulence
σ_C = turbulent Prandtl number for dissipation of turbulence
Γ = diffusion coefficient [kg/ms]
θ = dimensionless temperature
ϵ = dissipation of turbulent kinetic energy [m^2/s^3]
S_ϕ = source term

References

[1] **Law, H.S.** and **Masliyah, J.H.,** Mass Transfer Due to Confined Laminar Impinging Two Dimensional Jet, *Int. J. Heat Mass Transfer*, **27**: 529-539 (1984).

[2] **Chou, Y.J.** and **Hung, Y.H.,** Impinging Cooling of an Isothermally Heated Surface, *ASME J. Heat Transfer,* **116**: 479-482 (1994).

[3] **Lee, X.C., Xheng, Q., Zhung, Y.** and **Tia, Y.Q.,** Numerical Study of Recovery Effect And Impingement Heat Transfer With Submerged Circular Jets of Large Prandtl Number Liquid, *Int. J. Heat And Mass Transfer*, **40**: 2647-2653 (1997).

[4] **Behnia, M., Parneix, S., Shabany, Y.** and **Durby, P.A.,** Numerical Study of Turbulent Heat Transfer in Confined And Unconfined Impinging Jets, *Int. J. Heat Fluid Flow*, **20**: 1-9 (1999).

[5] **Cooper, D., Jackson, C., Launder, B.E.** and **Liao, G.X.,** Impingement Jet Studies For Turbulence Model Assessment-I Flow Field Experiments, *Int. J. Heat and Mass Transfer*, **36**: 2675-2684 (1993).

[6] **Park, T.S.** and **Sung, H.j.,** Development of Near Wall Turbulence Model and Application to Jet Impingement Heat Transfer*, Int. J. of Heat Fluid Flow*, **22**: 10-18 (2001).

[7] **Beitmal, A.H., Saad, M.A.** and **Patel, C.D.,** Effects of Surface Roughness on The Average Heat Transfer of An Impinging Air Jet, *International Communications in Heat and Mass Transfer*, **27**: 1-12 (2000).

[8] **Yang, Y.T.** and **Shyu, C.H.,** Numerical Study of Multiple Impinging Slot Jets With An Inclined Confinement Surface, *Numerical Heat Transfer*, Part A, **33**: 23-37 (1999).

[9] **EL-Gabry, Lamyaa, A.** and **Kamiski, Deborah, A**., Numerical Investigation of Jet Impingement With Cross Flow-Comparison of Yang-Shih And standard k-ϵ Turbulence Models, *Numerical Heat Transfer,* Part A, **47**: 441-469 (2005).

[10] **Craft, T.G., Graham, L.G.W.** and **Launder, B.E.,** Impinging Jet Studies For Turbulence Model Assessment-II- An Examination of The performance of Four Turbulence Models*, Int. J. Heat and Mass Transfer*, **36**: 2685-2697 (1993)

[11] **Shou Shing Hsieh, Jung-Tai Huang** and **Huang-Hsiu Tsai,** Impingement Cooling in A Rotating Square Annular Duct With Cross Flow Effect From Rib-Roughened Surface, *J. Heat and Mass Transfer*, **39** (2003).

[12] **Webb, R.L., Eckert, E.R.G.** and **Goldsten, R.J.,** Heat Transfer and Friction in Tubes With Repeated Rib Roughness, *International Journal of Heat and Mass*, **14**: 601-617 (1984).

[13] **Lio, T.M., Hwang, G.G.** and **Chen, S.H.**, Simulation and Measurements of Enhanced Turbulent Heat Transfer in Channels With Periodic Ribs on One Principal Wall, *International Journal of Heat Mass Transfer*, **36**: 507-507 (1993).

[14] **Rau, G., Cakan, M., Moeller, D.** and **Arts, T.,** The Effect of Periodic Ribs on The Local Aerodynamics and Heat Transfer Performance of A Straight Cooling Channel, *ASME Journal of Turbomachinery,* **120**; 368-375 (1988).

[15] **Han, J.C.,** Heat Transfer and Friction Characteristics in Rectangular Channels With Rib Turbulators, *ASME Journal of Heat Transfer*, **110**: 91-98 (1988).

[16] **Saidi, A.** and **Sunden, B.,** Numerical Prediction of Turbulent Convection Heat Transfer in Square Ribbed Ducts, *Numerical Heat Transfer*, Part A, **38**: 67-88 (2000).

[17] **Viswanathan, A.k.** and **Tafti, D.K.,** Detached Eddy Simulation of Turbulent flow and Heat transfer in Ribbed Duct, *ASME Journal of Fluid Engineering*, **127**: 888-896 (2005).

[18] **Viswanathan, A.k.** and **Tafti, D.K.,** Detached Eddy Simulation of Turbulent Flow and Heat transfer in Two-Pass Internal Cooling Duct, *International Journal of Heat and Fluid Flow*, **27**: 1-20 (2006).

[19] **Murtadha, A.** and **Mochizuki, S.**,Large Eddy Simulation With A Dynamics Sub Grid-Scale Model of Turbulent Flow in Orthogonally Rotating Rectangular Duct With Transverse Rib Turbulators, *International Journal of Heat Transfer*, **43**: 1243-1259 (2001).

[20] **Watanabe, K.** and **Takahashi, T.** (2002). Large eddy simulation of fully developed ribbed channel flow and heat transfer*, Proc. ASME Turbo Expo, 2002-GT-30203*.

[21] **Ichimiya, K.** and **Hosaka, N**., Experimental Study of Heat Transfer Characteristics Due To Confined Impinging Two Dimensional Jet*, Exp. Thermal and Fluid Science*, **5**: 803-807 (1992).

[22] **Launder, B.E.** and **Spalding, D.B.,** Lectures in Mathematical Model of Turbulence, Academic Press, London and NewYork, (1972).

[23] **Versteege, H.K.** and **Malalasekera, W.,** *An Introduction of Computational Fluid Dynamics*, Hemisophere Publishing Corporation, United State of America (1995).

تحليل الجريان الاضطرابي وانتقال الحرارة للتبريد التصادمي في مجرى هوائي بوجود جريان متقاطع

خضير سالم مشتت

كلية الهندسة- جامعة ذي قار- ناصرية - العراق

المستخلص. في هذا البحث أنجزت دراسة عددية لتحليل خصائص الجريان الاضطرابي وانتقال الحرارة للمنافث التصادمية في مجرى هوائي مع وجود جريان متقاطع. تضمنت الدراسة اختبار حالتين بالنسبة للمجرى الهوائي واحدة لمجرى بدون عوارض والأخرى لمجرى مع عوارض. تم تحليل خصائص الجريان وانتقال الحرارة تحت تأثير عوامل مختلفة، مثل: حجم المنافث، وعدد المنافث، وعدد العوارض، وسمك العارض، والمسافة بين المنافث، وعدد رينولدز للمنفث. استخدمت طريقة الحجم المحدد لتكامل معدلات الاستمرارية، ونافير ستوكس، والطاقة، حيث تعطي هذه الطريقة مجموعة من المعادلات الصحيحة للمجال الحسابي الكلي. عولجت تأثيرات الاضطراب باستخدام نموذج k-ϵ، بينما تأثير الجدار عولج باستخدام تقريب دالة الجدار. بينت النتائج أن حجم مناطق إعادة التدوير وتغير عدد نسلت الموضعي والطاقة الحركية للاضطراب قد تأثر بصورة كبيرة مع تغير حجم المنافث، وعدد المنافث والعوارض، والمسافة بين المنافث، وسمك العارض، وعدد رينولدز للمنفث. أيضا بينت النتائج أن ترتيب العوارض بالنسبة لموقع المنافث له تأثير واضح على زيادة معدل انتقال الحرارة. تم التأكد من صحة النتائج الحالية من خلال المقارنة مع النتائج العملية المنشورة.